Effect of mixing conditions and montmorillonite content on the mechanical properties of a chloroprene rubber

EFFECT OF MIXING CONDITIONS AND MONTMORILLONITE CONTENT ON THE MECHANICAL PROPERTIES OF A CHLOROPRENE RUBBER

M. Bakar,[1*] M. Przybyłek,[1] A. Białkowska,[1] W. Żurowski,[1] B. Hanulikova,[2] and R. Stoček[2]

[1]*University of Technology and Humanities, Chrobrego 27, 26-600 Radom, Poland*

[2]*Tomas Bata University, Trída Tomáše Bati 5678, 76001 Zlín, Czech Republic*

[*]*Corresponding author; e-mail: mbakar@wp.pl*

The effect oforganomodified montmorillonite (MMT) content and mixing conditions on the mechanical properties, structure, and morphology of a chloroprene rubber was investigated. Nanoparticles were mechanically mixed with a plasticizer, followed by ultrasonic homogenization before compounding of all ingredients ofthe mixtures in two-roll mills. Mechanical tests were carried out on samples prepared with three sonication amplitudes and containing different amounts of montmorillonite. The tensile strength and energy to break were found to increase by 15 and 70%, respectively, at the highest nanoclay content but the crack growth rate and tearing energy decreased. Variations in the mixing amplitude and MMT content did not influence the DSC and TGA thermograms, confirming an unchanged thermal stability of the nanocomposites. The highest sonication amplitude led to rubber mixtures with more uniform and homogeneous morphologies, with clay nanoparticles well dispersed and embedded in the rubber matrix.

Keywords: Rubber nanocomposites, mechanical properties, fatigue resistance, structure, morphology

Introduction

Due to their specific properties, elastomeric materials and their nanocomposites have attracted great interest in the last few decades. Various studies have confirmed that the properties of polymer nanocomposites depend not only of the properties and amount of their base components, but also on their preparation methods [**1-6**]. The preparation of rubber/ clay nanocomposites include the molten state [**7-12**], latex compounding [**13-15**] and the solution method [**16-18**]. The melt mixing has emerged as the most appropriate process for the preparation of rubber nanocomposites mainly because there is no need for a solvent. To obtain desired physical properties, only uniform dispersion of nanoparticles in the rubber matrix is required. Kim et al. [**7**] prepared nanocomposites based on a polybutadiene rubber and montmorillonite by the melt-compounding method. The results obtained showed that their abrasion resistance and the tensile and tear strengths were several times higher than those of a neat rubber. The rebound resilience, compression set, and abrasion resistance were also improved upon nanoclay addition. The enhanced mechanical properties were attributed to the presence of intercalated and exfoliated nanoclay particles in the rubber matrix, which was confirmed by a transmission electron microscopy analysis. Natural rubber nanocomposites based on an octadecylamine-modified bentonite, with a fully exfoliated structure and uniformly dispersed nanoparticles in the matrix, were prepared in [**8**] via a vulcanization process. It was found that the crosslinking degree of elastomer increased in the presence of organoclay, as corroborated by swelling

measurements and supported by a thermal analysis. Wu et al. **[9]** prepared natural rubber (NR), styrene-butadiene rubber (SBR), and ethylene-propylene-diene rubber (EPDM) nanocomposites by the melt blending process using an octadecylamine-modified fluorohectorite (OC). The tensile strength of SBR/OC and EPDM/OC nanocomposites containing 10 phr of OC, owing to their well ordered intercalated structure, was 4-5 times higher than that of the unmodified rubber. However, the NR/ OC nanocomposite exhibited an intermediately intercalated, and even exfoliated, structure. In another study, Wang and Wang [**10**] prepared styrene butadiene styrene (SBS) triblock copolymer nanocomposites by melt compounding prior to a morphology analysis and mechanical testing. The tensile stress, the strain at break, and the tearing strength of the SBS nanocomposites increased with nanoparticle content. The improvement in their mechanical properties was attributed to the relatively strong interface interaction between the copolymer and nanoparticles. A morphology analysis using scanning electron microscopy revealed an exfoliated structure of nanoparticles.

Although rather more complex, the latex mixing technique has also been widely used for the preparation of rubber-based nanocomposites [**13-15**]. Wu et al. [**14**] prepared different nanocomposites based on the styrene butadiene rubber (SBR), natural rubber (NR), nitrile butadiene rubber (NBR), and carboxylated acrylonitrile butadiene rubber (CNBR) by directly co-coagulating the rubber latex and an aqueous clay suspension. XRD patterns and TEM micrographs confirmed their unique structure, with separated layers, but without intercalation. The glass-transition temperature of SBR nanocomposites was higher than that of virgin SBR. Nanocomposites based on NR and SBR were prepared with an unmodified montmorillonite (Na^+ -MMT) by using the latex blending method [**15**]. The results obtained showed that the addition of 6 phr Na^+ -MMT improved the tensile strength and Young's modulus by 54 and 200%, respectively, in comparison with those of unfilled NR. SBR nanocomposites also showed improved mechanical properties and good thermal stability.

Other research groups have compared the properties of rubber nanocomposites prepared by different methods [**16-18**]. Lopez-Manchado et al. [**16**] prepared natural rubber nanocomposites with improved exfoliation by swelling organophilic layered silicates in an elastomer solution prior to compounding. The addition of a silane coupling agent during swelling led to a further improvement in the measured properties. An excellent dispersion of nanofillers in rubber compounds based on the BR or the SBR was also achieved by swelling the organophilic silicates in a rubber/toluene solution [**17**]. Liang et al. [**18**] compared the properties and morphology of isobutylene-isoprene rubber-based nanocomposites prepared by solution or melt intercalation methods. The nanocomposites exhibited outstanding mechanical characteristics and improved gas barrier properties, which was attributed to the nanometer-scale dispersion and the high aspect ratio of clay layers. However, the properties of nanocomposites prepared by solution intercalation were somewhat superior to those prepared by melt intercalation. Moreover, Smail and Ramli [**19**] used mechanical and solution mixing methods to prepare and study the properties of NR modified by nanoclay. Their results showed changes in the rheological properties, and the NR nanocomposites prepared by mixing in a solution had better mechanical properties than those prepared by the mechanical mixing. In the study of Magaraphan et al. [**20**], different amounts of organomodified montmorillonite nanoclay were successfully mixed with a solution of natural rubber in toluene. As a result, a fully exfoliated structure with improved mechanical properties at a nanoclay content below 10 phr was obtained.

TABLE 1. Ingredients Used to Prepare Rubber Formulations

Ingredients	Weight, kg			
Chloropren S-40		2.0		
f_M, %	0	1	2	3
Sulfur		0.57		
Nanoclay dispersion:				
Cloisite 20A	—	0.020	0.040	0.060
Santicizer 261A	—	0.067	0.134	0.200
Santicizer 261A	0.200	0.133	0.066	—
Zinc oxide		0.08		
Stearine		0.01		

The purpose of the present investigation was to prepare and evaluate the tensile properties and fatigue resistance of chloroprene filled with an organomodified Cloisite 20 montmorillonite. The dispersion of nanoparticles was carried out in the formulation plasticizer by using different sonication amplitudes.

1. Experimental

1.1. Materials

The following ingredients were used for the synthesis of elastomer nanocomposites:

- Chloroprene S 40, obtained from Versalis, San Donato Milanese, Italy;
- Cloisite 20 A, layered nanoclays modified with dimethyl dehydrogenated tallow and quaternary ammonium chloride, a Southern Clay Product;
- Santicizer 261A, (phthalate alkyl (C7-C9) benzyl) - plasticizer purchased from Brenntag Co. Kędzierzyn Koźle, Poland;
- Zinc oxide, white powder used as an accelerator, produced by “Huta Będzin”, Poland;
- Stearine, a mixture based on stearic and palmitic acids, manufactured by POCH S.A, (Gliwice, Poland);
- Brown factice, product obtained from unsaturated vegeTable oils with sulfur, produced by Kodrewex Company (Gomunice, Poland)
- Chalk, used as a filler, produced by Polcalc (Łódź, Poland);
- Wax (Protector G 35 WP) produced by Paramelt BV Costerstraat, Netherlands;
- Aflux, tetramethylthiuram disulfide used as a plasticizer, produced by Radka Co., Miekinia, Blonie, Poland;
- Accelerator T and accelerant DM (disulfide benzotriazole), purchased from Radka Co. (Miękinia-Błonie, Poland);
- Sulfur, a cross-linking substance produced by Siarkopol (Tarnobrzeg, Poland).

1.2. Preparation of rubber nanocomposites

First, different amounts of Cloisite 20A montmorillonite (1, 2, and 3 wt.%) were mechanically mixed with the Santicizer plasticizer during 10 min at room temperature, followed by ultrasonic homogenization with a UP200H apparatus Hielshermodel at different amplitudes (162, 216, and 270 μm) for 15 min. Plasticization of the mixtures was carried out at 50-60°C by using industrial roll mills.

The nanoparticles content and ultrasonic amplitude (with a constant dispersion time of 10 min) were varied to achieve optimum dispersion conditions and ultimate properties. The main ingredients of the formulations prepared are shown in **Table 1**.

1.3. Evaluation of mechanical properties

The tensile properties (tensile strength, strain at break, and energy to break) were evaluated on dumbbell-shaped specimens 2 mm thick at a strain rate of 200 mm/min, according to the PN-ISO 37:2007 standard, by using an Instron 5566 machine. Five samples were used for each data point.

The tear resistance was determined on rectangular samples, in accordance with the PN-ISO 34-1: 2007 standard, at a deformation rate of 100 mm/min using the same tensile machine.

Fatigue measurements was performed using a Tear and Fatigue Analyzer (Coesfeld GmbH, Germany). The fatigue crack growth and tearing energies were evaluated for different formulations and sonication amplitudes. The Paris-Erdogan equation, determining the fatigue crack growth *da / dn* in relation to the tearing energy E_T , is expressed as [**21**]

$$\frac{da}{dn} = bE_T^m, \qquad (1)$$

where *b* and *m* are material constants.

The tearing energy E_T is defined as the change in the deformation energy owing to the energy necessary for the creation of a new crack surface, namely,

$$E_T = -\frac{dW}{dA} = -\frac{dW}{B \cdot da}, \qquad (2)$$

where *W* is the recoverable elastic strain energy, *B* is sample thickness, and da is the crack length increment.

1.4. Characterization of structure and morphology

- A Fourier transform infrared (FTIR) analysis was performed on a Nicolet iN10 (Thermo Scientific, USA) spectrometer recording the IR spectra from 4000 to 760 cm^{-1}. The test was carried out in the ATR mode with a Germanium crystal.
- Differential scanning calorimetry (DSC) measurements were carried out on ~10-mg samples by using LabSys Evo DTA/DSC (Setaram, France) in a nitrogen atmosphere. The samples were

scanned from room temperature to 250°C, then cooled to 30°C, and finally heated to 250°C at the same rate of 10°C/min.

- A thermogravimetric analysis (TGA) was performed on the same apparatus as DSC in the temperature range of 30 -800°C in a nitrogen atmosphere at a heating rate of 10°C/min.
- The morphology of the rubber composites was investigated by a NovaNano SEM 450 (FEI company, The Netherlands) scanning electron microscope operating in a high vacuum mode at 3.0 kV.

2. Results and Discussion

2.1. Mechanical properties

Figure 1 shows the effect of montmorillonite (MMT) weight content fM and sonication amplitude *A* on the tensile strength σ_t of chloroprene rubber. Various studies have already demonstrated that the mechanical properties of polymer nanocomposites depend on nanofiller type, content, and dispersion conditions [**22-30**]. From **Fig. 1**, it is seen that the maximum tensile strength was reached at 3 wt.% MMT and the highest sonication amplitude. The improved properties of sonicated samples are generally explained by the good nanofiller dispersion in the rubber matrix and the specific interaction between the polymer matrix and incorporated nanoparticles. Moreover, an efficient stress transfer from stretched polymer chains to the nanoparticles also improves the measured properties.

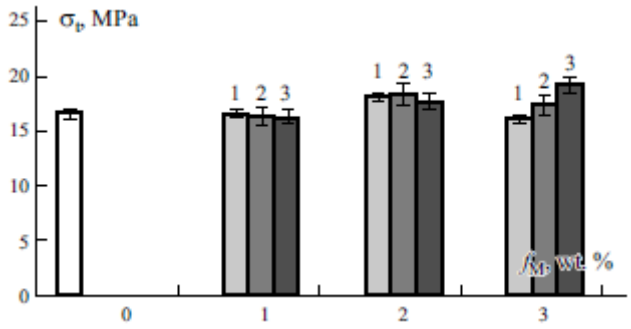

Fig. 1. Effect of montmorillonite (MMT) content f_M and sonication amplitude *A* on the tensile strength σ_t of chloroprene rubber: *A* = 162 (1), 216 (2), and 270 μm (3).

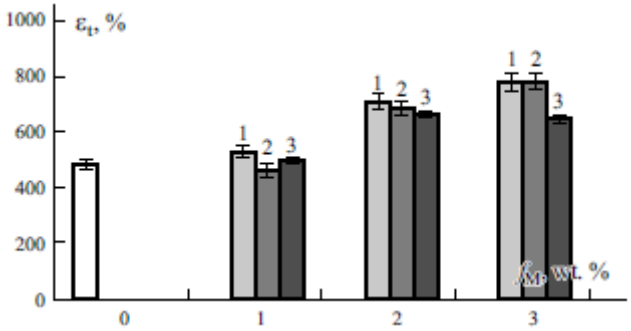

Fig. 2. Effect MMT content f_M and sonication amplitude *A* on the tensile strain ε_t at break of chloroprene rubber: *A* = 162 (1), 216 (2), and 270 (3) μm.

It is well known that the good properties of polymer nanocomposites arise because of the large interfacial polymer-nanolayer surface and the presence of large contact points in the interfacial region.

The ultrasound mixing is considered as the most powerful method to uniformly disperse agglomerated nanoparticles. It may induce some physical and chemical changes in substances exposed to ultrasound radiation. Hence, it is logical to consider the duration and amplitude of the sonication process as the key parameters for dispersion of nanoparticles in a polymer matrix. The sonication process has been used in various investigations to improve the nanoparticles dispersion during the polymer melt processing. Intermediate levels of mixing duration and sonication amplitude were found to give a proper dispersion of nanoparticles and better results [**4, 22**]. Moreover, Frasca et al. [**23**] demonstrated that the mechanical properties of rubber nanocomposites prepared by using ultrasonically assisted solution mixing procedure followed by two-roll milling were significantly improved compared with those of nanocomposites mixed only on a mill. The enhancement of mechanical and thermal properties of polymer nanocomposites is generally attributed to the intercalation of polymer chains between nanoclay layers [**5-7, 9-12**].

The tensile strain ε_t at break of chloroprene rubber is shown in **Fig. 2** as a function of montmorillonite (MMT) content f_M and sonication amplitude A . The value of ε_t was markedly higher for the rubber nanocomposites with 2 and 3 wt.% MMT, but it was not affected at 1 wt.% MMT. Moreover, the sonication amplitudes of 216 (80% of the highest amplitude) and 270 μm (the highest amplitude) led to the maximum increase in ε_t equal to about 60% compared with that of control samples.

TABLE 2. Tensile Energy W at Break and Modulus at a 300% Strain E of Chloroprene as a Function of MMT Content f_M and Sonication Amplitude A

f_M, wt. %	W, 10^3·kJ/m^2			E, MPa		
	A, μm					
	162	216	270	162	216	270
0	1.5 ± 0.1	1.5 ± 0.1	1.5 ± 0.1	2.48 ± 0.04	2.48 ± 0.04	2.48 ± 0.04
1	1.9 ± 0.1	1.55 ± 0.08	1.59 ± 0.12	2.48 ± 0.22	2.43 ± 0.13	2.40 ±0.36
2	2.64 ± 0.15	2.6 ± 0.2	2.48 ± 0.21	1.60 ± 0.02	1.69 ± 0.08	1.7 ± 0.1
3	2.5 ± 0.3	2.78 ± 0.07	2.6 ± 0.1	1.39 ± 0.08	1.47 ± 0.06	2.03 ± 0.07

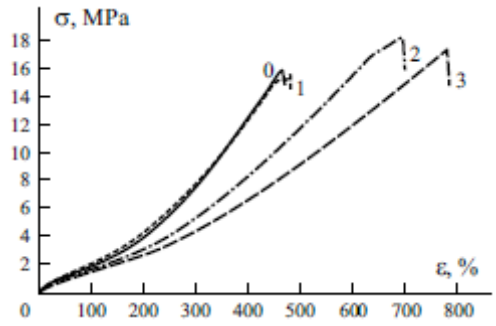

Fig. 3. Stress-strain curves of rubber samples with f_M = 0 (0), 1 (1), 2 (2), and 3 (3) wt.% mixed at A = 216 μm.

Numerous studies have confirmed that polymer nanocomposites require a specific mixing time and sonication amplitude to optimally improve their mechanical and thermal properties [**24 -28**].

Baig et al. [**25**] investigated the dispersion of graphene nanoplatelets (GNPs) in organic solvents by varying the sonication time and energy at three different amplitudes. It was found that high-intensity

sonication mixing led to defect formation and exfoliation phenomena. Moreover, the fragmentation of GNPs and defect formation increased with sonication time and amplitude. Tarawneh et al. [**31**] investigated the effect of mixing time and ultrasound on the mechanical properties of thermoplastic natural rubber (TPNR) nanocomposites. Results showed that, the tensile properties nanocomposites were improved owing to their combined intercalated-exfoliated structure. In addition, the optimum ultrasonic mixing time led to a good dispersion of the nanoclay platelets in the rubber matrix, which also improved the compatibility of the components.

The effect of montmorillonite content and sonication amplitude on the flexural energy at break and modulus were measured at a strain of 300%, and results are summarized in **Table 2**. The energy at break was determined from the area under load-displacement curves. The stress-strain curves of rubber samples containing different amounts of MMT and mixed at a sonication amplitude of 216 μm are shown in **Fig. 3**. The rubber nanocomposite with f_M = 3 wt.% showed the highest strain at break.

For comparison, the measured energy at break and modulus of the virgin rubber compound are also indicated. It is seen that maximum energy at break exhibited the rubber compound containing 3 wt.% of MMT and submitted to an intermediate sonication amplitude of 216 μm. The greatest growth in the energy at break, of about 85% compared with that for the unmodified rubber, can be associated with the increased tensile strength (**Fig.1**) and the strain at break (**Fig.2**).

The secant modulus (at a 300% strain) decreased with increasing amount of MMT, most probably, owing to the plasticizing effect of compounds associated with weakening of the intermolecular interaction. Several studies have also revealed the plasticization of polymer matrices by the pendants of alkyl ammonium chains [**32-34**]. Hanemann and Szabó [**32**] found that the incorporation of spherical nanoparticles led to the plasticization of the composites by depression of its glass-transition temperature.

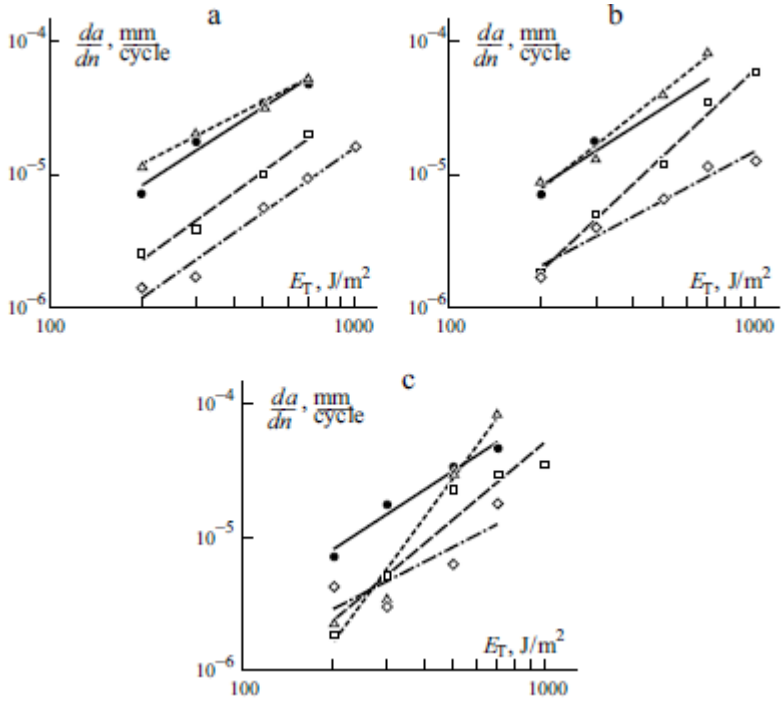

Fig. 4. Tearing energy E_T vs. crack growth rate da / dn for samples mixed at A = 162 (a), 216 (b), and 270 (c) μm. Dots are experimental data and lines are approximations by Eq. (1) at f_M = 0 (•, —), 1 (Δ, - - -), 2 (□, - - -), and 3 wt.% (◊, - , -).

In a separate study, it was found that the quaternary ammonium ions, apart from catalyzing the epoxy curing reactions, led to plasticization of a cross-linked matrix. In [**33**], a great reduction in the glass-transition temperature and storage modulus of cured epoxy networks were observed near the clay platelet surface due to the reduced cross-linking density. Similar results were obtained in study [35] dealing with the mechanical properties of rubber nanocomposites.

The experimental tearing energy E_T vs. crack growth rates *da / dn* for all prepared elastomer nanocomposites samples are presented by dots in **Fig. 4**, but values of the material constants *b* and *m* are summarized in **Table 3**. We should note that the crack growth rate *da / dn* can be fitted linearly (lines in **Fig. 4**) to the tearing energy E_T , which means that the experimental fatigue data can be properly described by power-law equation (1).

We should note that all analyzed samples showed a similar crack growth. The lowest concentration of nanoparticles had a negative influence on the fatigue resistance of all rubber nanocomposites in the sense that the crack growth rate in them was slightly higher than in unmodified samples. But, at higher values of f_M , the crack growth rate decreased with growing f_M . This may be explained by the additional cross-linking induced during the compounding process of rubber mixtures. Furthermore, we should mention that the slope of the crack growth rate-tearing energy curve, increased for the first MMT weight content f_M in the following order: A (A = 162 μm) < B (A = 216 μm) < C (A = 270 μm). For the second MMT content, this order was A < C < B, but for the last content — C < B < A, which is opposite to that for the rubber with the minimum MMT content. Thus, it can be said that the fatigue crack growth performance of an MMT-modified rubber will increase with amount of MMT.

TABLE 3. Constants *b* and m of Eq. (1) at Various Mixing Amplitudes *A* and MMT Weight Contents f_M and the Correlation Coefficient R^2

A, μm	f_M, wt. %	b	m	R^2
	0	$4 \cdot 10^{-9}$	1.4425	0.9704
162	1	$2 \cdot 10^{-8}$	1.1996	0.9925
	2	$4 \cdot 10^{-10}$	1.603	0.9829
	3	$2 \cdot 10^{-10}$	1.5987	0.9722
216	1	$3 \cdot 10^{-10}$	1.8736	0.9704
	2	$2 \cdot 10^{-11}$	2.1770	0.9915
	3	$2 \cdot 10^{-9}$	1.2692	0.9516
270	1	$2 \cdot 10^{-13}$	2.9818	0.9570
	2	$3 \cdot 10^{-11}$	2.0594	0.9273
	3	$8 \cdot 10^{-8}$	0.7342	0.7035

It is worth mentioning that the standard deviation is low when R^2 is very high. In such cases, the value predicted by a model is close to experimental data. The rather low value R^2 = 0.7035 of the correlation coefficient observed in one case pointed to the worst relative fitting of experimental data, could be caused by the formation of aggregates. The fitting is considered acceptable if $R^2 > 0.7$ **[36]**. In our case, the rubber compound modified with 3 wt.% MMT exhibited the slowest crack growth rate, confirming its rather high crack resistance. The fracture resistance of a nanocomposite decreases if the elastic energy at the crack tip is sufficiently high to propagate the crack. Nie et al. **[37]** attributed the improved resistance of a nanoparticle-modified natural rubber to crack growth to a better exfoliation and orientation of nanoclay layers. Yan et al **[38]** investigated the fatigue crack propagation in a natural

rubber containing graphene. Results showed that, in rubber nanocomposites, the crack growth was accelerated at lower fatigue strains and was retarded at higher strains. Authors explained this behavior by the competition between the strain-induced crystallization and cavitation at crack tips.

From the data of **Table 3**, one can see that the rubber nanocomposite containing 3 wt.% MMT and mixed at the highest amplitude A had the lowest value of the coefficient m, which points to the lowest crack growth rate at the given tearing energy and the highest resistance to the fatigue crack propagation.

2.2. Structure and morphology

Figure 5 depicts the fingerprint region of FTIR spectra of the chloroprene nanocomposites studied [**39, 40**]. The bands that can be found in the spectra correspond to the components used for nanocomposite preparation, mainly chloro-prene, Cloisite 20A (MMT), and Santicizer (C7-C9 alkyl-benzyl phthalate plasticizer). The bands representing polychlo-roprene are as follows: 3050-2840 cm-1 stretching of CH groups; 1660 cm^{-1} — stretching of the C=C alkene group, which is substituted by chlorine; double band; 1445-1425 cm^{-1} deformation of CH2; 820 and 775 cm^{-1} deformation of CH from HClC=C< tetrasubstituted group. MMT is represented by bands with the wavenumbers 3600-3000 cm^{-1}, attributed to stretching of the OH group; 1120-1010 cm^{-1} stretching of Si-O groups. Bands of the lower intensity belong to alkyl-benzyl phthalate, e.g., 1730 cm^{-1} — stretching of C=O groups and 1285 cm^{-1} — stretching of C-O group of this aromatic ester. As can be seen, the 1050-1010 cm^{-1} bands are most affected by the conditions during ultrasonication of rubber mixture. In the case of samples A (the lowest amplitude of ultrasonic mixing), there was no significant change in spectral band intensities in the whole range of wavenumbers. The spectra of samples B3 (rubber nanocomposite containing 3 wt.% MMT and mixed at A = 216 μm) and C3 (nanocomposite containing 3 wt.% of MMT and mixed at A = 270 μm) had highly intense MMT bands, which could mean that, at high mixing amplitudes, nanoparticles are arranged near the sample surface.

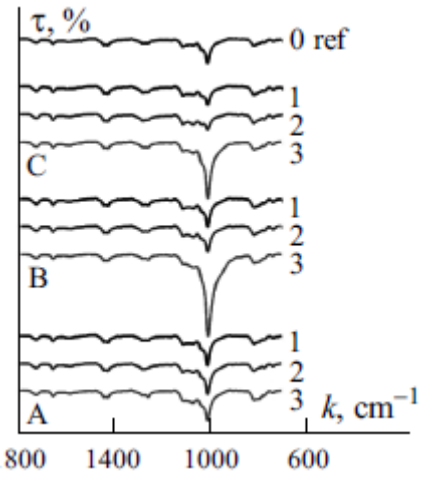

Fig. 5. FTIR spectra (transmittance t vs. wavenumber k) of samples with f_M = 0 (0), 1 (1), 2 (2), and 3 wt.% (3) at the sonication amplitudes A = 162 (A), 216 (B), and 270 (C) μm.

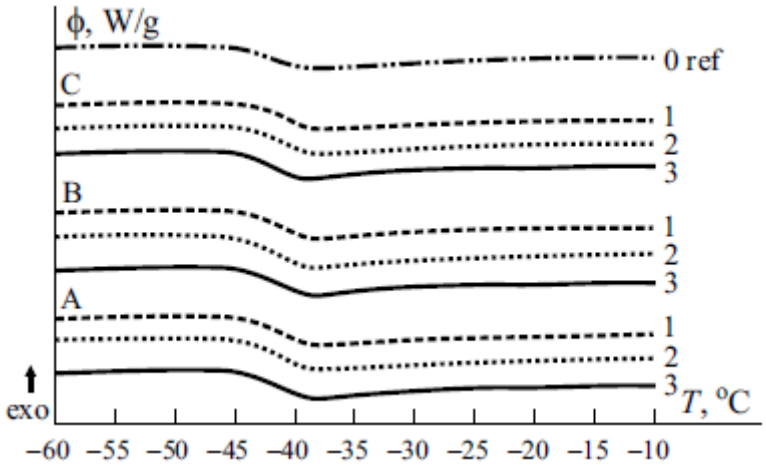

Fig. 6. DSC thermograms (heat flow 0 vs. temperature *T*) of rubber samples with f_M = 0 (- · -), 1 (- - -), 2 (···), and 3 wt.% (—) at *A* = 162 (A), 216 (B), and 270 (C) μm.

This is corroborated by the fact that the ATR method, which was used for the collection of FTIR spectra, analyzes the surface layer of samples. Another one can be the more homogenous exfoliation of nanoparticles between chloroprene chains at a higher MMT content f_M .

Figure 6 presents DSC thermograms of rubber compounds containing different amounts f_M of nanoparticles mixed at different sonication amplitudes *A* . The glass-transition temperatures t_g showed very similar trends, without significant differences in the temperature range from -41 to -43°C. The addition of organomodified MMT did not change the glass-transition temperatures of elastomer nanocomposites.

The weight loss of the rubber samples containing different MMT contents f_M and mixed at different sonication amplitudes *A* are exhibited in **Fig. 7**, and the data obtained are summarized in **Table 4**. As in the case of DSC results, there was no noticeable effect of added nanoparticles or sonication amplitudes on the weight loss or thermal stability of the nanocomposites.

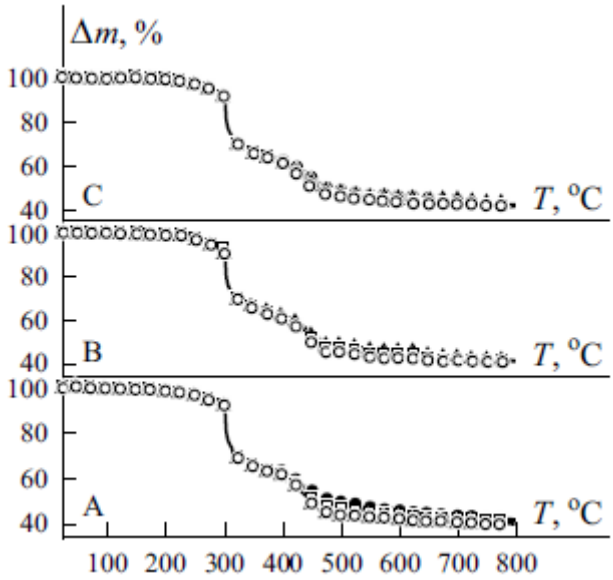

Fig. 7. Weight loss w of rubber samples with f_M = 0 (—•—), 1 (—□—), 2 (—Δ—), and 3 wt.% (—◊—) at *A* = 162 (A), 216 (B), and 270 (C) μm.

TABLE 4. DSC and Weight Loss Data

A, μm		162			216			270		
f_M, %	0	1	2	3	1	2	3	1	2	3
T_g, °C	–43	–42	–42	–42	–42	–43	–42	–41	–42	–43
t_d^1, °C	254	253	250	250	253	249	251	257	251	253
t_d^2, °C	301	302	299	300	301	299	299	303	301	300
t_d^3, °C	448	443	441	442	440	442	442	442	440	443
Δm_1, %	6	6	6	6	6	6	6	6	5	6
Δm_2, %	29	29	29	29	29	28	30	29	29	29
Δm_3, %	23	23	24	24	22	24	24	23	23	24
Δm, %	58	58	59	59	58	59	59	59	57	59

From Fig. 7 and results of **Table 4**, it is seen that all samples exhibited similar behavior when heated to 800°C in a nitrogen atmosphere. There can be found three degradation zones, 249-254°C (t^1_d), 299-303°C (t^2_d) and 440-448°C (t^3_d), which correspond to weight losses of 5-6% (Δm_1), 28-30% (Δm_2, the main degradation step), and 22- 24% (Δm_3), respectively. The total weight loss (Δm) was in the range 57-59 %.

The SEM micrographs of rubber mixtures containing different amounts f_M of montmorillonite (1% for A1, B1, C1), (2% for A2, B2, C2), (3% for A3, B3, C3) and mixed using three sonication amplitudes A (A, corresponding to A = 162 μm; B, corresponding to A = 216 μm; C, corresponding to A = 270 μm) are shown in **Fig. 8**.

It is seen that the reference rubber nanocomposite based on the unmodified rubber exhibited a wavy surface. However, the analyzed fracture surfaces of the samples seem to be quite homogeneous indicating that the selected mixing parameters and assigned preparation conditions have been rather appropriate. It is known that nanoparticles uniformly dispersed in a polymeric matrix, including the rubber matrix, have a significant effect on the mechanical and thermal properties of the relevant nanocomposites. Due to their high surface area, nanoparticles have a tendency to form aggregates, which can be eliminated, or at least reduced, by creating appropriate processing conditions.

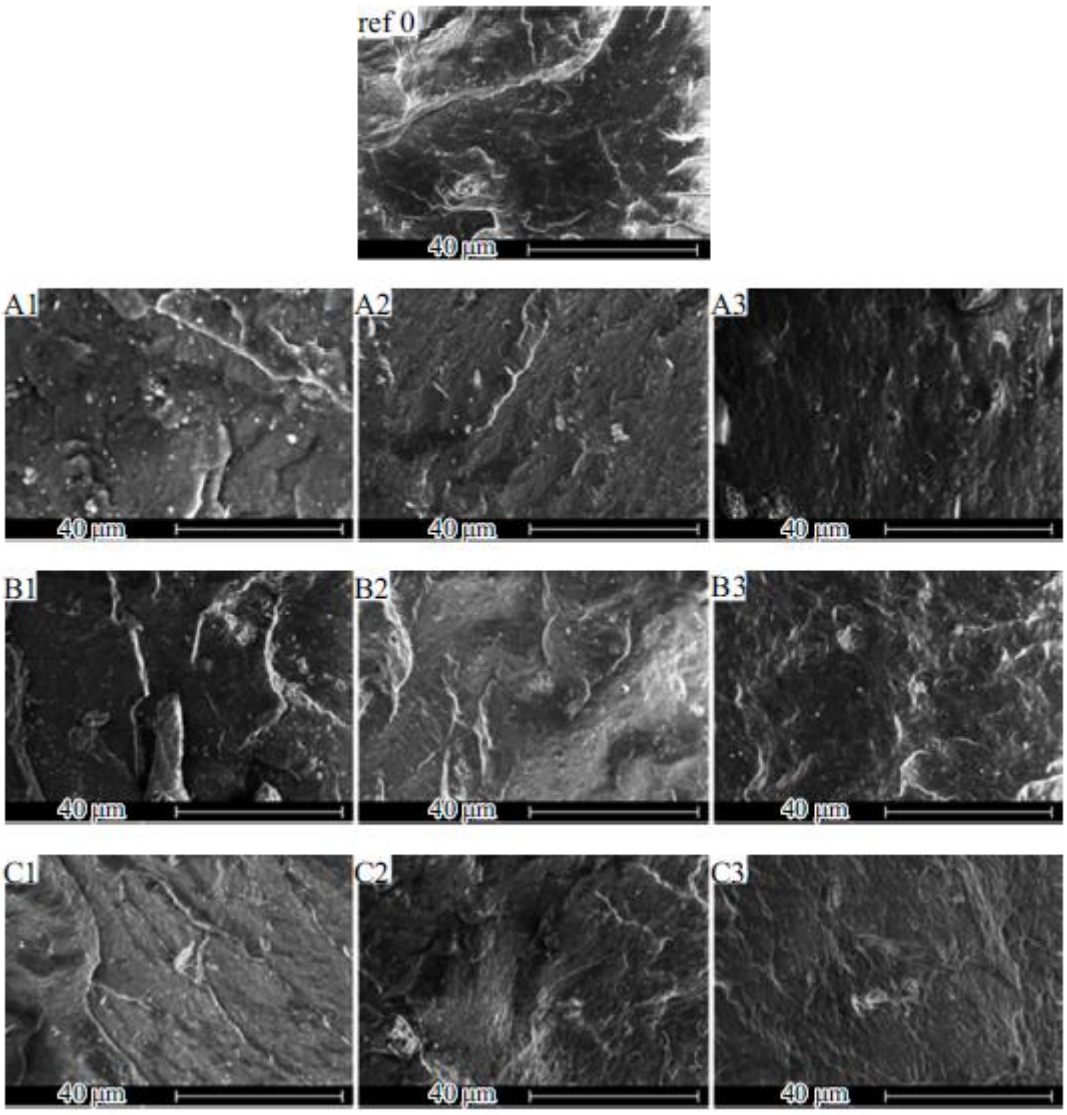

Fig. 8. SEM micrographs of rubber mixtures containing different amounts f_M of MMT and mixed at different sonication amplitudes A . Explanations in the text.

It has been shown that a better dispersion of nanoclay platelets can be achieved at their higher content than at lower ones. Moreover, it can be noted that the highest sonication amplitude lead to rubber nanocomposites with more uniform and homogeneous morphologies owing to the significant amount of energy supplied to rubber samples.

3. Conclusions

Chloroprene rubber nanocomposites with improved properties have been successfully prepared using nanoparticles homogenized and dispersed in the plasticizer of the formulations considered. The results obtained showed that the maximum increase in the tensile strength and strain at break, reaching 15 and 60%, respectively compared with those the control rubber sample, was exhibited by rubber compound containing 3 wt.% MMT and submitted to the highest sonication amplitude (i.e., 270 µm). A higher amount of MMT led to their better dispersion in the rubber nanocomposites than lower ones.

Nanocomposite samples with more uniform and homogeneous morphologies and improved mechanical properties were obtained at the highest sonication amplitude and highest energy supplied to the mixtures. The crack growth rate was fitted linearly to the tearing energy by the Paris-Erdogan power-law equation. The rubber nanocomposite containing 3 wt.% MMT and prepared with the highest sonication amplitude showed the lowest crack growth rate, making it the most resistant to fatigue crack propagation. This was explained by to the positive effect of the additional cross-linking induced during the compounding process of the rubber and by the improved compatibility between nanoclay nanoparticles and the rubber matrix.

A FTIR spectra analysis showed an increased nanofiller band, probably caused by a more homogenous exfoliation of nanoparticles. According to a DSC analysis, the glass-transition temperatures had a very similar trend, without significant differences in the range from -41 to -43°C. SEM micrographs indicated that the nonmodified rubber mixture had a wavy surface and that a better dispersion of nanoclay can be achieved with a higher amount of nanoclay.

REFERENCES

1. S. Thomas and R. Stephen, Rubber Nanocomposites: Preparation, Properties, and Applications, John Wiley & Sons, New York-Chichester-Brisbane-Toronto (2010).
2. M. Galimberti, Rubber-Clay Nanocomposites: Science, Technology, and Applications, John Wiley & Sons, New York-Chichester-Brisbane-Toronto (2011).
3. D. Feldman, “Elastomer nanocomposite properties,” J. Macromol. Sci. A, 49, No. 9, 784-793 (2012).
4. L. Bokobza, “Natural rubber nanocomposites: a review,” Nanomaterials, 9, No. 12, 1-21 (2019).
5. G. A. Forental, S. B. Sapozhnikov, and A. A. Dyakonov, “Physicomechanical characteristics of an elastomeric composite containing silicon oxide nanoparticles with account of interface layer,” Mech. Compos. Mater., 51, No. 3, 341-346 (2015).
6. S. Amirchakhmaghi, A. A. Nia, G. Azizpour, and H. Bamdadi, “The effect of surface treatment of alumina nanoparticles with a silane coupling agent on the mechanical properties of polymer nanocomposites,” Mech. Compos. Mater., 51, No. 3, 347-358 (2015).
7. M. S. Kim, D. W. Kim, S. Ray Chowdhmy, and G. H. Kim, “Melt-compounded butadiene rubber nanocomposites with improved mechanical properties and abrasion resistance,” J. Appl. Polym. Sci., 102, No. 3, 2062-2066 (2006).
8. M. A. Lopez-Manchado, B. Herrero, and M. J. P. I. Arroyo, “Preparation and characterization of organoclay nanocomposites based on natural rubber,” Polym. Int., 52, No. 7, 1070-1077 (2003).
9. Y. P. Wu, Y. Ma, Y. Q. Wang, and L. Q. Zhang, “Effects of characteristics of rubber, mixing and vulcanization on the structure and properties of rubber/clay nanocomposites by melt blending,” Macromol. Mater. Eng., 289, No. 10, 890894 (2004).

10. Z. Wang and X. Wang, “Preparation and mechanical properties of styrene-butadiene-styrene triblock copolymer/partly exfoliated montmorillonite nanocomposites prepared by melt compounding,” J. Thermoplast. Compos. Mater., 24, No. 1, 83-95 (2011).

11. Y. W. Chang, Y. Yang, S. Ryu, and C. Nah, “Preparation and properties of EPDM/organomontmorillonite hybrid nanocomposites,” Polym. Int., 51, No. 4, 319-324 (2002).

12. H. N. Azlina, H. A. Sahrim, and R. Rozaidi, “Effect of nanoclay on the microstructure and the properties of thermoplastic natural rubber (TPNR)/OMMT nanocomposites,” J. Thermoplast. Compos. Mater., 25, No. 3, 351-362 (2012).

13. S. Varghese and J. Karger-Kocsis, “Natural rubber-based nanocomposites by latex compounding with layered silicates,” Polymer, 44, No. 17, 4921-4927 (2003).

14. Y. P. Wu, Y Q. Wang, H. F. Zhang, Y Z. Wang, D. S. Yu, L. Q. Zhang, and J. Yang, “Rubber-pristine clay nanocomposites prepared by co-coagulating rubber latex and clay aqueous suspension,” Compos. Sci. Technol., 65, No. 7-8, 1195-1202 (2005).

15. S. Mitra, S. Chattopadhyay, and A. K. Bhowmick, “Preparation and characterization of elastomer-based nanocomposite gels using an unique latex blending technique,” J. Appl. Polym. Sci., 118, No. 1, 81-90 (2010).

16. M. A. Lopez-Manchado, B. Herrero, and M. Arroyo, “Organoclay-natural rubber nanocomposites synthesized by mechanical and solution mixing methods,” Polym. Int., 53, No. 11, 1766-1772 (2004).

17. M. Ganter, W. Gronski, P. Reichert, and R. Mulhaupt, “Rubber nanocomposites: morphology and mechanical properties of BR and SBR vulcanizates reinforced by organophilic layered silicates,” Rubber Chem. Technol., 74, No. 2, 221-235 (2001).

18. Y. Liang, Y Wang, Y. Wu, Y Lu, H. Zhang, and L. Zhang, “Preparation and properties of isobutylene-isoprene rubber (IIR)/clay nanocomposites,” Polym. Test., 24, No. 1, 12-17 (2005).

19. H. Ismail and R. Ramli, “Organoclay filled natural rubber nanocomposites, The effects of filler loading and mixing method,” J. Reinf. Plast. Compos., 27, No. 16-17, 1909-1924 (2008).

20. R. Magaraphan, W. Thaijaroen, and R. Lim-Ochakun, “Structure and properties of natural rubber and modified mont-morillonite nanocomposites,” Rubber Chem. Technol., 76, No. 2, 406-418 (2003).

21. P. Paris and F. Erdogan, “A critical analysis of crack propagation laws,” J. Basic Eng., 85, No. 4, 528 -533 (1963).

22. G. Gkikas, N. M. Barkoula, and A. S. Paipetis, “Effect of dispersion conditions on the thermomechanical and toughness properties of multi walled carbon nanotubes-reinforced epoxy,” Composites, Part B, 43, No. 6, 2697-2705 (2012).

23. D. Frasca, D. Schulze, V. Wachtendorf, M. Morys, and B. Schartel, “Multilayer graphene/chlorine-isobutene-isoprene rubber nanocomposites: the effect of dispersion,” Polym. Adv. Technol., 27, No. 7, 872-881 (2016).

24. J. R. Potts, O. Shankar, S. Murali, L. Su, and R. S. Ruoff, “Latex and two-roll mill processing of thermally-exfoliated graphite oxide/natural rubber nanocomposites,” Compos. Sci. Technol., 74, 166-172 (2013).

25. Z. Baig, O. Mamat, M. Mustapha, A. Mumtaz, K. S. Munir, and M. Sarfraz, “Investigation of tip sonication effects on structural quality of graphene nanoplatelets (GNPs) for superior solvent dispersion,” Ultrason. Sonochem., 45, 133-149 (2018).

26. M. S. Goyat, S. Ray, and P. K. Ghosh, “Innovative application of ultrasonic mixing to produce homogeneously mixed nanoparticulate-epoxy composite of improved physical properties,” Composites Part A, 42, No. 10, 1421-1431 (2011).

27. B. Bittmann, F. Haupert, and A. K. Schlarb, “Preparation of TiO2/epoxy nanocomposites by ultrasonic dispersion and their structure property relationship,” Ultrason. Sonochem., 18, No. 1, 120-126 (2011).

28. M. Watanabe, J. Ikeda, Y Takeda, M. Kawai, and T. Mitsumata, “Effect of Sonication Time on Magnetorheological Effect for Monomodal Magnetic Elastomers,” Gels, 4, No. 2, 49 (2018).

29. C. Pina-Hernandez, L. Hernández, L. M. Flores-Velez, L. F. Del Castillo, and O. Dominguez, “Processing and mechanical properties of natural rubber-ZnFe2O4 nanocomposites,” J. Mater. Eng. Perform., 16, No. 4, 470-476 (2007).

30. M. Bhattacharya, M. Maiti, and A. K. Bhowmick, “Influence of different nanofillers and their dispersion methods on the properties of natural rubber nanocomposites,” Rubber Chem. Technol., 81, No. 5, 782-808 (2008).

31. M. A. A. Tarawneh, S. H. Ahmad, R. Rasid, S. Y. Yahya, and S. Y. E. Noum, “The enhancement of properties of TPNR/ clay nanocomposites using ultrasonic treatment,” J. Reinf. Plast. Compos., 30, No. 6, 524-532 (2011).

32. T. Hanemann and D. VSzabó, “Polymer-nanoparticle composites: from synthesis to modern applications,” Materials, 3, No. 6, 3468-3517 (2010).

33. J. Park and S. C. Jana, “Effect of plasticization of epoxy networks by organic modifier on exfoliation of nanoclay,” Macromolecules, 36, No. 22, 8391-8397 (2003).

34. R. L. Zhang, L. F. Zhao, Y. D. Huang, and L. Liu, “Effect of silane coupling agent on the mechanical properties of nitrile butadiene rubber (NBR)/organophilic montmorillonite (OMMT) nanocomposites,” Sci. Eng. Compos. Mater., 23, No. 3, 277-282 (2016).

35. M. Przybyłek, A. Białkowska, M. Bakar, U. Kosikowska, and T. Szymborski, “Effect of aging conditions on the mechanical properties and antimicrobial activity of elastomer nanocomposites,” J. Polym. Eng., 39, No. 4, 316-325 (2019).

36. M. Balachandran, S. Devanathan, R. Muraleekrishnan, and S. S. Bhagawan, “Optimizing properties of nanoclay-nitrile rubber (NBR) composites using Face Centred Central Composite Design,” Mater. Des., 35, 854-862 (2012).

37. Y. Nie, L. Qu, G. Huang, B. Wang, G. Weng, and J. Wu, “Improved resistance to crack growth of natural rubber by the inclusion of nanoclay,” Polym. Adv. Technol., 23, No. 1, 85-91 (2012).

38. N. Yan, H. Xia, Y Zhan, and G. Fei, “New insights into fatigue crack growth in graphene-filled natural rubber composites by microfocus hard-X-ray beamline radiation,” Macromol. Mater. Eng., 298, No. 1, 38-44 (2013).

39. G. Socrates, Infrared and Raman Characteristic Group Frequencies, John Wiley & Sons, New York, 3rd edition (2001).

40. L. Alexandrescu, M. Ficai, L. F. Albu, L. E. C. A. Minodora, and M. Mihut, “Influence of montmorillonite nanoparticles on polychloroprene adhesive properties,” Leather Footwear J., 13, No. 1, 61 (2013).